iJRASET
International Journal For Research in Applied Science and Engineering Technology

INTERNATIONAL JOURNAL FOR RESEARCH

IN APPLIED SCIENCE & ENGINEERING TECHNOLOGY

Volume: 13 **Issue:** XII **Month of publication:** December 2025

DOI: https://doi.org/10.22214/ijraset.2025.76019

www.ijraset.com

Call: 08813907089 | E-mail ID: ijraset@gmail.com

International Journal for Research in Applied Science & Engineering Technology (IJRASET)
ISSN: 2321-9653; IC Value: 45.98; SJ Impact Factor: 7.538
Volume 13 Issue XII Dec 2025- Available at www.ijraset.com

Static, Modal, and Harmonic Response Analysis of the Connecting Rod–Piston Assembly for the Honda Supra Engine Using FEM

Valentin Mereuta
Faculty of Engineering, University "Dunarea de Jos", Galati, Romania

Abstract: ***This study presents a finite element method (FEM) analysis of the connecting rod - piston assembly used in internal combustion engines. The study includes static, modal, and harmonic response analyses to evaluate the structural integrity and dynamic behavior of the assembly under realistic operating conditions. The static analysis investigates the distribution of stresses and deformations under the maximum pressure in the combustion chamber, verifying the strength and stiffness of the components, while the modal analysis determines the natural frequencies and mode shapes, which are essential for avoiding resonance phenomena. The harmonic response analysis evaluates the dynamic behavior under periodic excitations, highlighting critical frequencies where vibrational amplification may occur. The results show that the assembly has adequate structural stiffness, stable dynamic behavior with natural frequencies outside the engine's operational range, as well as effective damping properties, ensuring durability and reliability. This integrated FEM approach provides a solid foundation for optimizing the design and performance of engine components subjected to complex loads.***

Keywords: FEM analysis, Solid modeling, Autodesk Inventor, Ansys Workbench

I. INTRODUCTION

Engine pistons are among the most complex and important components of an internal combustion engine. The function of the piston is to withstand the gas pressure and to enable the rotation of the crankshaft through the connecting rod, which is responsible for transferring the force generated by the piston to the crankshaft, so that the reciprocating motion of the piston is converted into rotary motion by the crankshaft.

The piston operates under high temperature, high pressure, high speed, and poor lubrication conditions. It is subjected to cyclic gas pressure and inertial forces, and these severe operating conditions may lead to fatigue failure such as piston skirt wear, cracking of the piston crown, and other defects. A piston in an internal combustion engine must meet the following requirements: sufficient strength to resist gas pressure; minimum weight; ability to reciprocate with minimal noise; adequate bearing area to prevent wear; effective dissipation of heat generated during combustion; and good resistance to distortion under high loads and temperatures.

There are various materials and manufacturing methods used for producing connecting rods, which are subjected to high compressive loads due to combustion as well as tensile loads due to inertia. A high cyclic load in the range of 10^8 to 10^9 cycles acts on the connecting rod [1].

Tensile and compressive stresses are generated by gas pressure, while bending stresses result from centrifugal effects and eccentricity. Therefore, the connecting rod is typically designed with an I-shaped cross-section to ensure minimum weight and maximum rigidity [2]. Consequently, the durability of the connecting rod is of critical importance.

Abhinav Gautam et al. [1] performed a static stress analysis of a connecting rod made of SS 304 stainless steel used in the Cummins NTA 885 BC engine. The model was developed in CATIA V5 and imported into ANSYS WORKBENCH 14.0. They reported that the region near the root of the small end of the connecting rod is highly prone to failure, most likely due to the high compressive load caused by the piston pin assembly.

B. Anusha et al. [3] conducted a static analysis of a Hero Honda Splendor connecting rod using ANSYS. The rod was modeled in PRO/E ic) and imported into ANSYS Workbench. Their results showed that maximum stress occurred at the piston end of the connecting rod and remained below the allowable stress limit of the material.

Mohammed et al. [4] described the cause of connecting rod failure using the finite element method with MSC Patran software and also performed a metallographic study of a buckled connecting rod. They reported that casting defects and porosity initiated and propagated cracks on the fractured surface.

Suraj Pal et al. [5] carried out a finite element analysis of a Hero Honda Splendor connecting rod using ANSYS Workbench. The model was created in Pro/E Wildfire 4.0. Static and fatigue analyses were performed to determine von Mises stress, shear stress, elastic strain, and total deformation. They concluded that the highest stresses occurred at the piston end, and therefore increasing the material in this region was recommended to reduce peak stresses.

Shahrukh Shamim [6] performed modeling and analysis of a connecting rod, focusing on material E-glass/Epoxy and Aluminium composite optimization. Their study addressed of aspects: von-Mises stress, Shear stress, total deformation and equivalent elastic strain for the given loading conditions.

Ram Bansal et al. [7] conducted a dynamic analysis of a connecting rod. The model of the single-cylinder, four-stroke diesel engine connecting rod was created using CATIA V5R18, and the analysis was performed in ANSYS Workbench.

For the static analysis, both traditional connecting rod materials and composite materials such as E-glass/Epoxy and aluminum nanocomposite reinforced with carbon nanotubes were considered.

Ms. Snehal B. Kambale et al. [8] designed and analyzed a connecting rod using composite materials. The 3D solid model was generated in NX software, and the finite element analysis was performed in ANSYS. The main objective of the study was to evaluate stresses and deformations when changing the material while maintaining the same geometry.

Anusha B. et al. (2013) analyzed and compared cast iron and structural steel connecting rods. The connecting rod was modeled in Pro/E and analyzed in ANSYS Workbench. The case study involved the Hero Honda Splendor connecting rod. A pressure of 3.15 MPa was applied at the piston end, and the big end was fixed. Structural steel exhibited lower stresses compared with cast iron and showed superior performance. The design was considered safe for both materials, but structural steel was recommended.

Rao G. N. M. (2013) compared steel, aluminum, titanium, and cast iron for potential weight-reduction applications. The results showed that the steel connecting rod experienced lower stress and deformation compared to titanium, cast iron, and aluminum.

Pathade V. C. et al. (2013) used three methods to investigate connecting rod stresses: finite element analysis, photoelasticity, and theoretical calculations. The photoelastic sheet was cast using resin AY103 and hardener HY951. The rod was modeled in Pro/E and analyzed in ANSYS Workbench 11.0. Stress concentration was observed at both ends, and negligible stress was found in the mid-section. Additionally, the small end experienced higher stresses than the big end.

Sarkate T. S. et al. (2013) performed a comparative study of Aluminum 7068 alloy and AISI 4340 alloy steel. Static analysis was conducted using Pro/E Wildfire 4.0 and ANSYS V12. The results showed a 63.95% weight reduction and a 3.59% decrease in stresses when using Aluminum 7068.

Singh R. (2013) studied two connecting rod materials: isotropic steel and orthotropic E-glass/Epoxy, conducting linear static FEA. The rod was modeled in CATIA V5R10 and analyzed in MSC.PATRAN. E-glass/Epoxy reduced stresses by 33.99% and displacement by 0.026%. The use of a TET-10 mesh was recommended for improved accuracy.

Kumar et al. (2012) used CAE tools for optimizing connecting rod parameters. The rod was modeled in Pro/E and analyzed in ANSYS Workbench 11.0. Loads were applied alternately at the small and big ends. Maximum stresses occurred at the piston end. The study recommended modifying geometric parameters, increasing material at the piston end, and using materials such as C-70 steel.

Pal et al. (2012) used FEA for design evaluation and optimization. The rod was modeled in Pro/E Wildfire 4.0 and analyzed in ANSYS V12. A weight reduction of 0.477 g was achieved, and the small end was found to be the most highly stressed region. Increasing material in critical areas was recommended to reduce stresses. Fatigue strength was highlighted as an important design parameter.

Pathade V. C. et al. (2012) performed theoretical and finite element analyses of an internal combustion engine connecting rod. The big end was fixed, and various loads were applied at the small end. They concluded that the small end experiences higher stresses than the big end.

Cioată et al. (2010) conducted a static analysis of the connecting rood. The model was developed in Autodesk Inventor and analyzed in ANSYS V11. A deformation of 0.036 mm was obtained using FEA and 0.073 mm using classical analytical methods. Their study emphasized the importance of using CAD and FEA tools in engineering analysis.

Muhammad Hilman Karem [18] developed various piston head geometries made of aluminum and magnesium alloys and used FEM analysis with ANSYS to evaluate the piston under static and transient conditions. The solid modeling of the piston was carried out in SOLIDWORKS software and subsequently exported to ANSYS WORKBENCH. According to the static analysis, it was found that the flat-head piston generates higher stresses compared with the rounded-head piston. A similar trend is observed in the transient analysis, where the rounded-head piston manages to maintain an almost constant stress level over time.

ISSN: 2321-9653; IC Value: 45.98; SJ Impact Factor: 7.538
Volume 13 Issue XII Dec 2025- Available at www.ijraset.com

II. CONNECTING ROD - PISTON ASSEMBLY

The assembly analyzed in this study consists of the connecting rod and piston, and also includes the wrist pin, rings, and retaining elements. The three-dimensional modeling of all components was carried out in Autodesk Inventor Professional 2026, using parameterized geometries to ensure dimensional accuracy and compatibility between parts. Both the connecting rod and the piston were accurately reconstructed based on the original design data. The final assembly structure Fig. 1, was validated geometrically and kinematically to reproduce real mounting conditions prior to export into the FEM analysis environment.

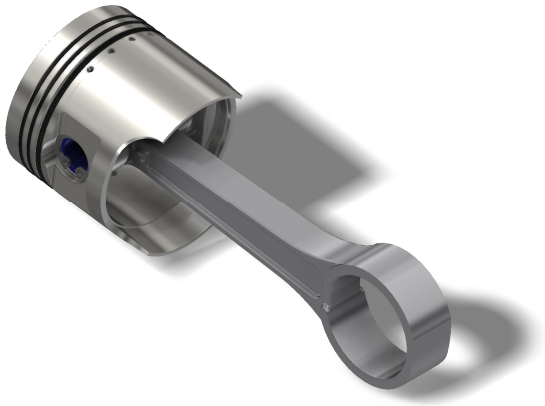

Fig. 1 3D connecting rod–piston assembly

III. STATIC ANALYSIS

The numerical investigations performed in this study include static, modal, and harmonic response analyses of the connecting rod–piston assembly. The static structural analysis aims to evaluate the stress distribution, strain fields, and resulting deformations under the maximum loading conditions expected during engine operation. Modal analysis is conducted to identify the natural frequencies and corresponding vibration modes of the assembly, as these parameters are essential for assessing the risk of resonant behavior. Additionally, a harmonic response analysis is carried out to determine the dynamic behavior of the system under cyclic excitation, providing insight into amplitude variations and potential fatigue-critical regions when subjected to operational engine frequencies. Together, these analyses offer a comprehensive understanding of the structural and dynamic performance of the assembly.

A. Choosing Material

The selection of materials for the components of the connecting rod–piston assembly was carried out based on mechanical performance requirements, manufacturability, and compatibility with real engine applications. The piston was modeled using AISI 12CuNiMg, an alloy steel known for its high strength, good wear resistance, and favorable thermal stability under cyclic loading. The connecting rod was assigned the material 42CrMo4, a widely used quenched-and-tempered alloy steel characterized by high fatigue strength and excellent toughness. The piston pin was designed using 40Cr, selected for its superior hardness and ability to withstand high contact stresses. The piston rings were modeled with 41Cr4, which provides a balanced combination of strength, elasticity, and wear resistance, essential for maintaining sealing performance. Finally, the retaining clips were assigned SAE 1950, ensuring sufficient resilience and dimensional stability under repeated assembly and service conditions. This material configuration ensures realistic mechanical behavior and supports an accurate FEM-based evaluation of the assembly. Materials and their properties are shown in Table 1.

TABLE I
MATERIAL PROPERTIES

Parameters	AISI12CuNiMg	42CrMo4 Alloy Steel	40Cr Steel	41Cr Steel	SAE1050 Steel
Young’s Modulus	75000	210000	210000	210000	210000
[MPa]	0.33	0.3	0.29	0.29	0.29
Poisson's Ratio	28190	80000	81390	81390	81390
Shear Modulus	2700	7850	7850	7850	7850
[MPa]	180	1100	400	800	500

Parameters	AISI12CuNiMg	42CrMo4 Alloy Steel	40Cr Steel	41Cr Steel	SAE1050 Steel
Mass Density [Kg/m^3]	300	950	700	1000	700
Tensile Strength [MPa]					
Yield Strength [MPa]					

B. The Restrictions and Load Condition

Within the finite element analysis methodology, the constraints and loads applied to the connecting rod–piston assembly were defined to reproduce the actual operating conditions inside the engine mechanism. The maximum combustion chamber pressure, with a value of 5.15 MPa, Fig. 2, was applied on the upper surface of the piston crown as a uniformly distributed load, representing the action of the gases generated during the combustion phase.

To accurately simulate the transfer of loads to the crankshaft, a Fixed Support condition was imposed at the big end of the connecting rod, corresponding to the rigid articulation in the crank pin bearing. The connections between the piston pin and the piston bosses, as well as between the pin and the small end of the connecting rod, were defined as mechanical contacts (bonded or frictional, depending on the scenario) to replicate the real interaction between components and to allow evaluation of local stress concentrations.

Additionally, gravity was applied to the entire assembly to account for the effect of self-weight on the stress and deformation distribution. Defining these boundary conditions ensures an accurate representation of the structural behavior of the assembly in the static, modal, and harmonic analyses presented in the following sections.

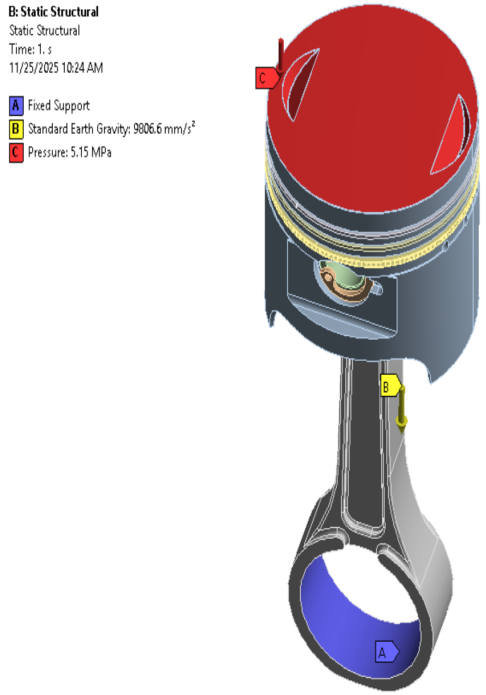

Fig. 2 Restrictions and load condition

C. Generate Meshing

For the discretization of the connecting rod - piston assembly, a tetrahedral element mesh was employed, suitable for the complex geometry of the components and the localized stress distribution. The global element size was set to 2 mm, while in critical regions, such as the piston head, the pin boss areas, and the small end of the connecting rod, a mesh refinement with 0.5 mm elements was applied in order to accurately capture the local variations of the stress and deformation fields.

The final finite element mesh consisted of 239225 nodes and 120535 elements, ensuring an optimal balance between result accuracy and computational cost, Fig. 3. This configuration allowed stable solution convergence for the static, modal, and harmonic analyses

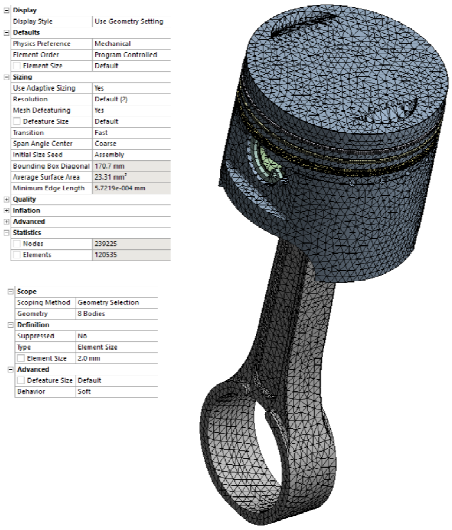

Fig. 3 Connecting rod–piston assembly meshing

D. Static Analysis Results

The results of the static analysis highlight the structural behavior of the connecting rod–piston assembly under the action of the maximum combustion chamber pressure and the other applied boundary conditions. The maximum deformation recorded in the assembly was 0.0712 mm, Fig. 4, occurring predominantly in the piston crown area and in the thin regions near the pin bosses. This value corresponds to a low elastic deformation, indicating adequate structural rigidity and confirming that the assembly can sustain the applied loads without excessive deflections that could affect the proper functioning of the mechanism.

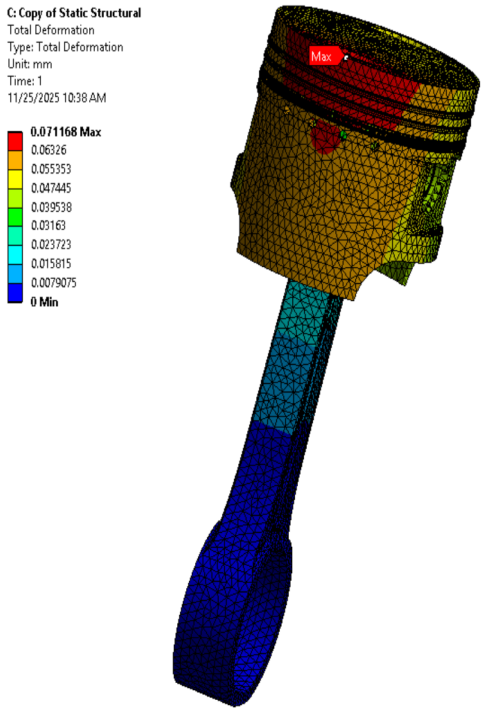

Fig. 4 Deformation of connecting rod–piston assembly

The distribution of equivalent Von Mises stresses shows a maximum value of 278.62 MPa, Fig. 5, concentrated in the small end of the connecting rod and in the contact region between the piston pin and the piston - areas known to be prone to high loading due to the cyclic transfer of forces. The magnitude of these stresses remains within the allowable limits of the selected materials, without exceeding their mechanical strength.

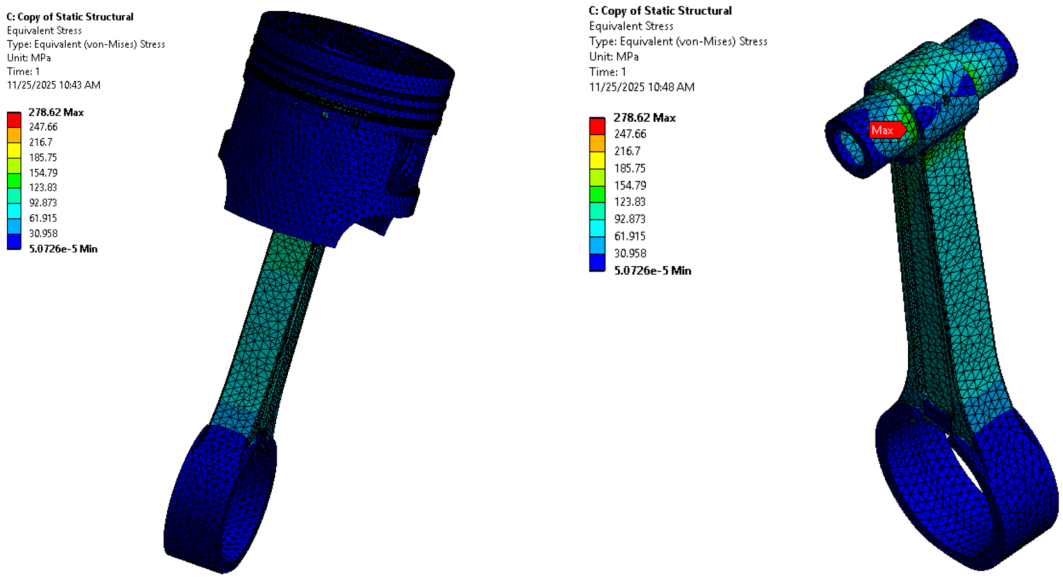

Fig. 5 Von Mises Stress of connecting rod - piston assembly

Based on these results, the computed Factor of Safety (FOS) for the assembly is 1.546, Fig. 6, indicating that the structure operates safely, with an additional margin of strength relative to the maximum loading conditions for which it was designed.

The obtained FOS confirms that the chosen geometry and materials are suitable for the applied loads and that the assembly exhibits a robust mechanical behavior under static loading.

Overall, the static analysis reveals a favorable distribution of stresses and deformations, with no indications of potential structural failure, providing a solid foundation for the subsequent stages of numerical evaluation, including modal and harmonic analysis.

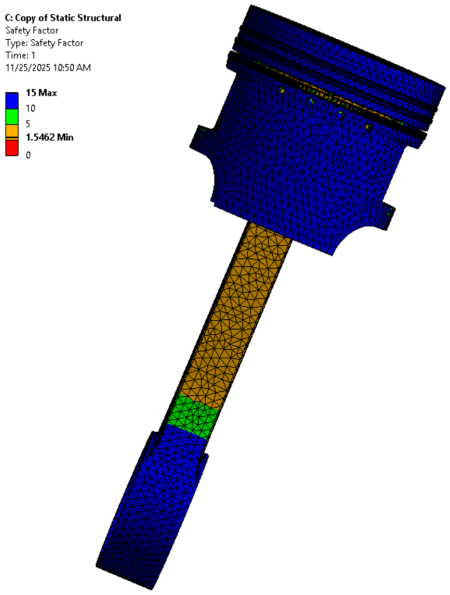

Fig. 6 Factor of Safety

E. Modal Analysis Results

The modal analysis of the connecting rod–piston assembly was conducted to identify the natural vibration frequencies and the corresponding mode shapes, which represent essential parameters for evaluating the dynamic behavior of the mechanism. Determining the natural modes is crucial for avoiding resonance phenomena, which may lead to vibration amplification, accelerated fatigue, and potential structural failure.

ISSN: 2321-9653; IC Value: 45.98; SJ Impact Factor: 7.538
Volume 13 Issue XII Dec 2025- Available at www.ijraset.com

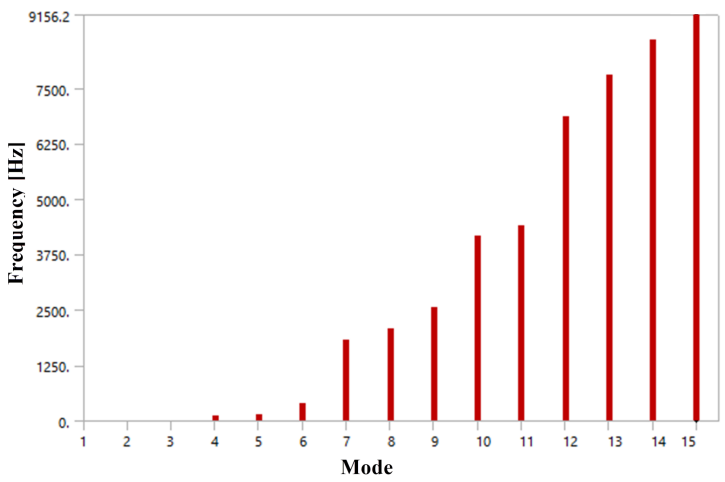

Fig. 7 Modal analysis results

Mode	Frequency [Hz]
1.	0.
2.	
3.	6.0886e-003
4.	123.11
5.	142.9
6.	383.63
7.	1816.5
8.	2085.1
9.	2550.2
10.	4164.3
11.	4398.1
12.	6857.9
13.	7798.6
14.	8583.5
15.	9156.2

Fig. 8 Natural vibration frequencies

The obtained results reveal a wide modal spectrum, corresponding to the high stiffness of the assembly and the local variation in component mass distribution, Fig. 7 and 8. The first mode, with a frequency of 0 Hz, corresponds to the rigid-body displacement of the assembly without structural deformation. A second rigid-body mode appears at very low frequency values, which is characteristic of assemblies composed of elements connected through multiple contact interfaces. The first deformable modes begin to occur at a frequency of approximately 0.006 Hz, indicating a very low level of flexibility in the overall structural configuration.

The dynamically relevant natural modes are located at higher frequencies, such as 123.11 Hz, 142.90 Hz, and 383.63 Hz, where localized deformations occur in regions of lower stiffness or near component interfaces. At higher frequencies - 1816.5 Hz, 2085.1 Hz, 2550.2 Hz, and reaching up to very high modes such as 9156.2 Hz - the mode shapes show localized deformations of the piston, the connecting rod, or oscillations of the piston pin relative to the piston bosses.

The resulting modal spectrum indicates that the first dynamically relevant natural modes are well above the frequency range characteristic of internal combustion engine operation (typically below 300 Hz for dominant vibrations). This confirms that the connecting rod–piston assembly possesses adequate structural rigidity and that the risk of resonance phenomena occurring during normal operating conditions is low.

In conclusion, the modal analysis demonstrates that the assembly exhibits stable dynamic behavior, with well-spaced natural modes and sufficiently high frequencies to avoid interference with the mechanical excitations generated during the engine cycle. These results support the structural robustness of the assembly and provide a solid foundation for subsequent harmonic analysis.

F. Harmonic Response Results

The Harmonic Response analysis was carried out in order to evaluate the dynamic behavior of the assembly under the application of a harmonic excitation within a frequency range between 66.67 Hz and 300 Hz. This analysis allows the determination of the evolution of the Von Mises stress amplitude and the phase angle with respect to frequency variation, contributing to the identification of potential critical frequencies at which the structure may exhibit amplified vibrational behavior.

The obtained results show that, in the low-frequency range (66.67–116.67 Hz), the stress amplitude gradually increases from 7.3062×10^{-3} MPa to an intermediate maximum value of 5.2447×10^{-2} MPa at 116.67 Hz. In this region, the phase angle remains constant at 0°, indicating an elastic-dominated response in which displacements and stresses are in phase with the external excitation. A significant change occurs around 133.33 Hz, where the phase angle shifts to 180°. This phase inversion is typical when passing through a region near a natural frequency or a point where the system's dynamic stiffness changes. The amplitude at this frequency decreases to 3.3957×10^{-2} MPa, followed by a sharp reduction as the frequency increases.

In the 150–300 Hz range, the stress amplitude progressively decreases from 8.0185×10^{-3} MPa to 9.5666×10^{-4} MPa, confirming a rigid-system behavior, with vibrational effects diminishing as the excitation moves away from the natural frequencies. In this region, the phase angle remains constant at 180°, indicating an inertia-dominated response, with stresses being out of phase with the applied excitation.

The Amplitude–Frequency graph, Fig. 9, confirms these observations, showing a pronounced peak at approximately 116.67 Hz, followed by a rapid decrease in amplitude after entering the inverted-phase regime. The absence of significant amplitude growth at higher frequencies suggests that the structure does not present resonance risks within the analyzed range.

In conclusion, the Harmonic Response analysis indicates a stable dynamic behavior, with a single major point of interest around 116–133 Hz. The low level of maximum amplitudes, remaining below 0.053 MPa, confirms that the structure is not prone to excessive vibrations within the studied frequency domain, supporting the robustness and reliability of the assembly under harmonic excitation.

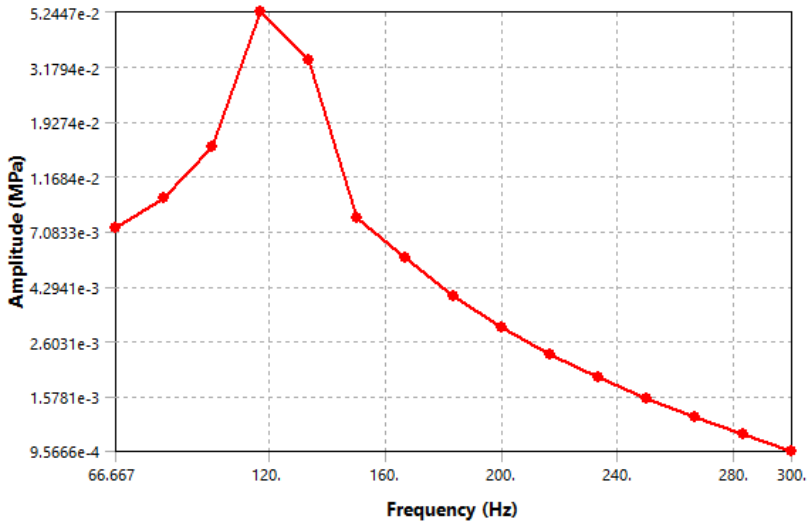

Fig. 9 Variation of stress amplitude as a function of the harmonic excitation frequency

The Harmonic Response analysis focused on evaluating the displacement amplitudes of the assembly was carried out over the same frequency interval, ranging from 66.67 Hz to 300 Hz, in order to determine the structural sensitivity to harmonic dynamic excitations. The objective of this stage was to identify possible frequencies at which the connecting rod–piston assembly may exhibit higher displacement amplitudes, which could influence the mechanism's operation or generate localized fatigue phenomena.

In the low-frequency range (66.67–116.67 Hz), the displacement amplitude gradually increases from 2.4518×10^{-3} mm to a distinct peak value of 2.0848×10^{-2} mm at 116.67 Hz. The phase angle remaining constant at 0° throughout this interval indicates a typical elastic behavior, in which the structural response is in phase with the harmonic excitation.

A significant change is observed at 133.33 Hz, where the amplitude slightly decreases to 1.8525×10^{-2} mm, while the phase angle undergoes a shift to 180°. This inversion is a classical indicator of approaching a natural frequency or of a transition in the dynamic stiffness characteristics, highlighting the shift in dominance between elastic and inertial components in the system's response.

For frequencies between 150 Hz and 300 Hz, the displacement amplitude exhibits a clear decreasing trend, reducing from 1.6532×10^{-3} mm to 2.7446×10^{-4} mm. Although the phase angle alternates between 0° and 180° in this region, the amplitudes remain low, indicating a typical rigid-body dynamic behavior in which inertial effects dominate.

The Amplitude–Frequency plot confirms the presence of a pronounced peak around 116.67 Hz, followed by a rapid attenuation after entering the phase-inverted regime. The absence of additional significant peaks within the analyzed frequency domain indicates that the structure does not exhibit resonance-related risks that could compromise its integrity.

Overall, the Harmonic Response analysis based on displacements, Fig. 10, demonstrates a stable dynamic behavior, revealing a single major point of interest in the vicinity of 116–133 Hz.

The low amplitude levels, remaining below 0.021 mm, confirm that the assembly is not susceptible to excessive vibrations under the investigated operating conditions, supporting the structural robustness and reliability of the mechanism under harmonic excitation.

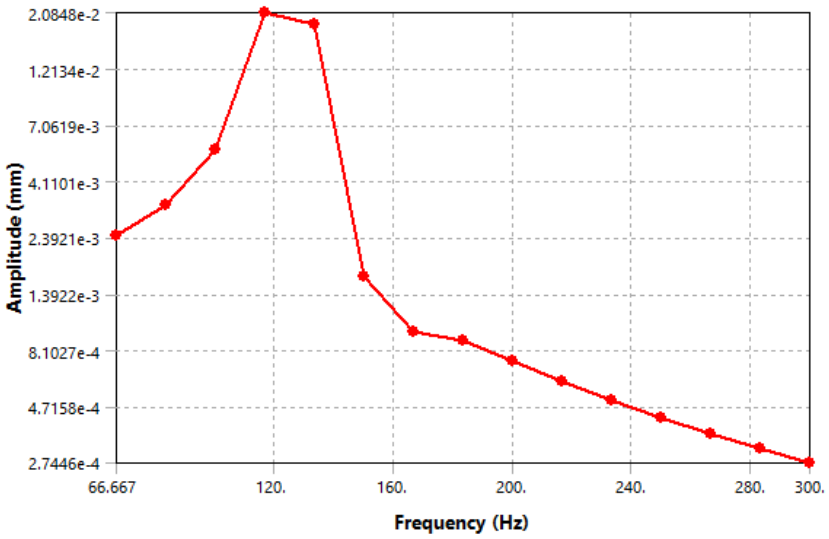

Fig. 10 Variation of displacement amplitude as a function of the harmonic excitation frequency

Comparing the two types of responses provides a comprehensive perspective on the dynamic stiffness of the system and on the regions susceptible to amplified vibrations.

Considering the behavior of amplitudes as a function of frequency, it is observed that both stresses and displacements exhibit a pronounced peak at nearby frequencies, around 116.67 Hz. For the Von Mises stresses, this value represents the global maximum ($\approx 5.24 \times 10^{-2}$ MPa), while for displacements the maximum also corresponds to the same frequency ($\approx 2.08 \times 10^{-2}$ mm). The presence of a common maximum indicates that the system is approaching a region of increased dynamic sensitivity, possibly due to proximity to a natural vibration mode.

However, the absolute amplitudes differ significantly between the two responses: stresses show variations more strongly influenced by local stiffness and material characteristics, while displacements reflect the global behavior of the assembly. This differentiation highlights the non-uniform distribution of stiffness within the assembly, especially at the piston head and the small end of the connecting rod.

When examining the phase angle, it is observed that a common feature of both responses is the phase inversion at 133.33 Hz, where the phase shifts from 0° to 180°. This phenomenon is typical of passing through a region close to resonance or of changes in the relationship between the elastic and inertial components of the structure.

Although the phase of both responses undergoes similar inversions, the magnitude of the amplitudes shows different behavior immediately after this frequency. The stresses decrease rapidly, confirming the structural stiffness that limits the transmission of dynamic loads at higher frequencies, whereas the displacements decrease more gradually, with a gentler slope, indicating the assembly's ability to dissipate vibrations.

In the higher frequency range (150–300 Hz), both quantities exhibit a decreasing trend: stresses drop from 8.0185×10^{-3} MPa to 9.5666×10^{-4} MPa, and displacements decrease from 1.6532×10^{-3} mm to 2.7446×10^{-4} mm.

This simultaneous reduction confirms the absence of other relevant natural modes within the analyzed domain and suggests that the assembly operates far from any potentially dangerous resonance in this frequency range.

Comparing the two responses shows that displacements are more sensitive to dynamic excitation near the first peak ($\approx$ 116 Hz), representing an indicator of the system's flexibility, while stresses exhibit similar peaks but are much more controlled, reflecting a good distribution of stiffness in the critical areas of the assembly.

The fact that both responses have a single significant maximum followed by a consistent decrease indicates the behavior of a well-designed system from a dynamic standpoint, with a single marked sensitivity zone and a well-damped resonance.

IV. CONCLUSION

The performed FEM analyses enabled a detailed evaluation of the structural and dynamic behavior of the connecting rod–piston assembly. The static analysis highlighted the distribution of stresses and deformations under operating loads, ensuring the verification of strength and stiffness, while the modal analysis identified the natural frequencies and vibration modes, which are fundamental for avoiding resonance phenomena. The harmonic response analysis allowed the assessment of dynamic behavior under periodic excitations, revealing critical zones of vibrational amplification and contributing to the optimization of the component's durability and reliability.

The static analysis of the connecting rod–piston assembly demonstrated appropriate structural stiffness, with satisfactory performance under the imposed loads, ensuring safe operation.

The modal analysis showed that the natural frequencies of the assembly lie above the normal operational range of the engine, indicating stable dynamic behavior and a reduced risk of resonance phenomena.

The harmonic response results confirmed the dynamic stability of the assembly, highlighting a single resonant sensitivity zone with low vibration amplitudes, reflecting good damping capacity. This indicates that the connecting rod - piston assembly exhibits robust and reliable behavior under both static and dynamic conditions, supporting the durability and optimal performance of the engine mechanism.

REFERENCES

[1] Gautam, K Priya Ajit, "Static Stress Analysis of Connecting Rod Using Finite Element Approach", IOSR Journal of Mechanical and Civil Engineering (IOSR-JMCE), Volume 10, Issue 1 (Nov. - Dec. 2013), PP 47-51, 2013.
[2] P. G. Charkha, S. B. Jaju, "Analysis & Optimization of Connecting Rod" Second International Conference on Emerging Trends in Engineering and Technology, ICETET-09, 2009.
[3] Anusha, C.Vijaya Bhaskar Reddy, "Modeling and Analysis of Two Wheeler Connecting Rod by Using Ansys", IOSR Journal of Mechanical and Civil Engineering (IOSR-JMCE), Volume 6, Issue 5 (May. - Jun. 2013), PP 83-87.
[4] Mohammed et al., "Failure Analysis of a Fractured Connecting Rod", Journal of Asian Scientific Research, vol. 2 issue 11, pp737-741, 2012.
[5] S. Pal et al., "Design Evaluation and Optimization of Connecting Rod Parameters Using FEM", International Journal of Engineering and Management Research, Vol.-2, Issue-6, December 2012, ISSN No.: 2250-0758, Pages: 21-25, 2012.
[6] Mr. S. Shamim, "Design and Comparative Analysis of Connecting Rod Using Finite Element Method", International Journal of Engineering Research & Technology (IJERT), ISSN: 2278-0181, Vol. 3 Issue 9, September- 2014.
[7] R. Bansal, "Dynamic Simulation of a Connecting Rod Made of Aluminium Alloy Using Finite Element Analysis Approach Method" IOSR Journal of Mechanical and Civil Engineering (IOSR-JMCE), Jan. - Feb. Vol 5, Issue 2, pp01-05, 2013.
[8] Ms. S. B. Kambale, Prof. M. P. Chopade, Dr. V. S. Goranttiwar, "Finite Element Analysis of Connecting Rod Using Composite Material", International Journal for Research in Applied Science & Engineering Technology (IJRASET), ISSN: 2321-9653; IC Value: 45.98; SJ Impact Factor: 7.538, Volume 10 Issue V May 2022- Available at www.ijraset.com, 2022.
[9] Anusha, C.V.B Reddy, "Modelling and Analysis of Two Wheeler Connecting Rod by Using ANSYS". IOSR-JMCE, Vol. 6, Issue 5, 2013.
[10] G.N.M. Rao, "Design Optimization and Analysis of Connecting Rod Using ANSYS" IJSR, Vol. 2, issue 7, 2013.
[11] C.V. Pathade, B. Patle, A.N. Ingale, "Stress Analysis of I. C. Engine Connecting Rod by FEM", International Journal of Engineering and Innovative Technology (IJEIT), Volume 1, Issue 3, March 2012.
[12] T.S. Sarkate, S.P. Washimkar, S.S. Dhulekar, "Optimization of Steel Connecting Rod by Aluminum Connecting Rod Using Finite Element Analysis", International Journal of Advance Research, Ideas and Innovations in Technology,Vol. 1, Issue 1, 2013.
[13] R. Singh, "Stress Analysis of Orthotropic and Isotropic Connecting Rod Using Finite Element Method", IJMERR, Vol. 2 No. 2, 2013.
[14] Kumar, K. Grover, B. Budania, "Optimization of Connecting Rod Parameters Using CAE Tools", IJLTET, Vol. 1, Issue 3, 2012.
[15] S. Pal, S. Kumar, "Design Evaluation and Optimization of Connecting Rod Parameters Using FEM". IJEMR, Vol. 2, issue 6, 2012.
[16] V.C. Pathade, D.S. Ingole, "Stress Analysis of I. C. Engine Connecting Rod by FEM and Photoelasticity", IOSR-JMCE, Vol 6, Issue 1, 2013.
[17] V.G. Cioata, I. Kiss, "Computer Aided Design of the Connecting Rod" Faculty of Technical Sciences Novi Sad, Machine Design, 2010.
[18] M.H. Karem, Al E. Ismail, "Finite Element Analysis of Piston for Structural Assessments", Journal of Sustainable and Manufacturing in Transportation" Vol. 1 No. 1 8-16, DOI: https://doi.org/10.30880/jsmt.2021.01.01.002.

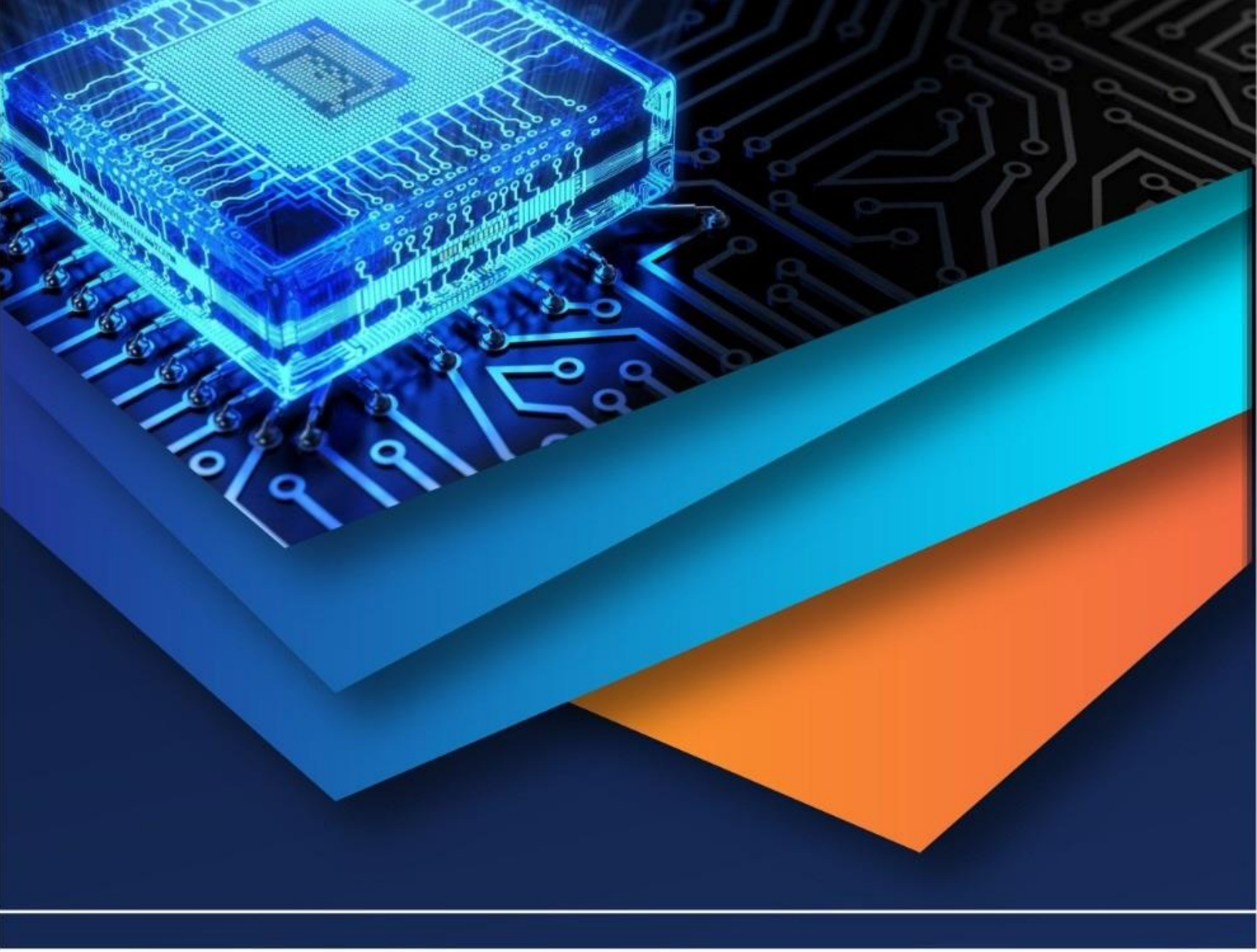

10.22214/IJRASET

45.98

IMPACT FACTOR: 7.129

IMPACT FACTOR: 7.429

INTERNATIONAL JOURNAL FOR RESEARCH

IN APPLIED SCIENCE & ENGINEERING TECHNOLOGY